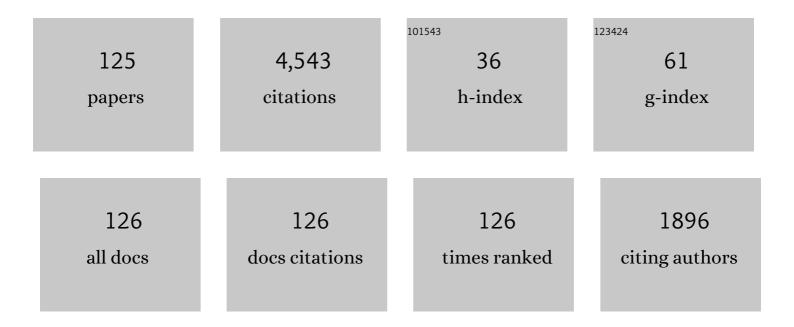
List of Publications by Year in descending order

Source: https://exaly.com/author-pdf/8634834/publications.pdf Version: 2024-02-01



OINCLAI FENC

#	Article	IF	CITATIONS
1	Closure of the East Paleotethyan Ocean and amalgamation of the Eastern Cimmerian and Southeast Asia continental fragments. Earth-Science Reviews, 2018, 186, 195-230.	9.1	231
2	Marine productivity changes during the end-Permian crisis and Early Triassic recovery. Earth-Science Reviews, 2015, 149, 136-162.	9.1	214
3	The end-Permian regression in South China and its implication on mass extinction. Earth-Science Reviews, 2014, 137, 19-33.	9.1	212
4	The protracted Permo-Triassic crisis and multi-episode extinction around the Permian–Triassic boundary. Global and Planetary Change, 2007, 55, 1-20.	3.5	202
5	Plankton and productivity during the Permian–Triassic boundary crisis: An analysis of organic carbon fluxes. Global and Planetary Change, 2013, 105, 52-67.	3.5	187
6	Earliest Triassic microbialites in the South China block and other areas: controls on their growth and distribution. Facies, 2007, 53, 409-425.	1.4	146
7	Time-calibrated Milankovitch cycles for the late Permian. Nature Communications, 2013, 4, 2452.	12.8	135
8	Negative C-isotope excursions at the Permian-Triassic boundary linked to volcanism. Geology, 2012, 40, 963-966.	4.4	101
9	Brachiopod miniaturization and its possible causes during the Permian–Triassic crisis in deep water environments, South China. Palaeogeography, Palaeoclimatology, Palaeoecology, 2007, 252, 145-163.	2.3	91
10	Evolution of oceanic redox conditions during the Permo-Triassic transition: Evidence from deepwater radiolarian facies. Earth-Science Reviews, 2014, 137, 34-51.	9.1	85
11	Radiolarian evolution during the latest Permian in South China. Global and Planetary Change, 2007, 55, 177-192.	3.5	81
12	Mercury enrichments provide evidence of Early Triassic volcanism following the end-Permian mass extinction. Earth-Science Reviews, 2019, 195, 191-212.	9.1	81
13	Proliferation of shallow-water radiolarians coinciding with enhanced oceanic productivity in reducing conditions during the Middle Permian, South China: evidence from the Gufeng Formation of western Hubei Province. Palaeogeography, Palaeoclimatology, Palaeoecology, 2016, 444, 1-14.	2.3	75
14	Two pulses of oceanic environmental disturbance during the Permian–Triassic boundary crisis. Earth and Planetary Science Letters, 2016, 443, 139-152.	4.4	71
15	Volcanism in South China during the Late Permian and its relationship to marine ecosystem and environmental changes. Global and Planetary Change, 2013, 105, 121-134.	3.5	70
16	Geochronological, elemental and Sr-Nd-Hf-O isotopic constraints on the petrogenesis of the Triassic post-collisional granitic rocks in NW Thailand and its Paleotethyan implications. Lithos, 2016, 266-267, 264-286.	1.4	70
17	Detrital zircon U-Pb-Hf isotopes and provenance of Late Neoproterozoic and Early Paleozoic sediments of the Simao and Baoshan blocks, SW China: Implications for Proto-Tethys and Paleo-Tethys evolution and Gondwana reconstruction. Gondwana Research, 2017, 51, 193-208.	6.0	70
18	Geochronological and geochemical constraints on the mafic rocks along the Luang Prabang zone: Carboniferous back-arc setting in northwest Laos. Lithos, 2016, 245, 60-75.	1.4	68

#	Article	IF	CITATIONS
19	Magmatic record of Prototethyan evolution in SW Yunnan, China: Geochemical, zircon U–Pb geochronological and Lu–Hf isotopic evidence from the Huimin metavolcanic rocks in the southern Lancangjiang zone. Gondwana Research, 2015, 28, 757-768.	6.0	65
20	Correlation of Triassic stratigraphy between the Simao and Lampang-Phrae Basins: implications for the tectonopaleogeography of Southeast Asia. Journal of Asian Earth Sciences, 2005, 24, 777-785.	2.3	60
21	A LATE CHANGHSINGIAN (LATE PERMIAN) DEEPWATER BRACHIOPOD FAUNA FROM THE TALUNG FORMATION AT THE DONGPAN SECTION, SOUTHERN GUANGXI, SOUTH CHINA. Journal of Paleontology, 2005, 79, 927-938.	0.8	59
22	Origin of volcanic ash beds across the Permian–Triassic boundary, Daxiakou, South China: Petrology and U–Pb age, trace elements and Hf-isotope composition of zircon. Chemical Geology, 2013, 360-361, 41-53.	3.3	59
23	Arc-like volcanic rocks in NW Laos: Geochronological and geochemical constraints and their tectonic implications. Journal of Asian Earth Sciences, 2015, 98, 342-357.	2.3	57
24	Mercury fluxes record regional volcanism in the South China craton prior to the end-Permian mass extinction. Geology, 2021, 49, 452-456.	4.4	57
25	Sponge spicules from the lower Cambrian in the Yanjiahe Formation, South China: The earliest biomineralizing sponge record. Palaeogeography, Palaeoclimatology, Palaeoecology, 2017, 474, 36-44.	2.3	52
26	Biogenic silica and organic carbon fluxes provide evidence of enhanced marine productivity in the Upper Ordovician-Lower Silurian of South China. Palaeogeography, Palaeoclimatology, Palaeoecology, 2019, 534, 109278.	2.3	52
27	Paleo-productivity evolution across the Permian-Triassic boundary and quantitative calculation of primary productivity of black rock series from the Dalong Formation, South China. Science China Earth Sciences, 2014, 57, 1583-1594.	5.2	49
28	Cambrian intra–oceanic arc trondhjemite and tonalite in the Tam Ky–Phuoc Son Suture Zone, central Vietnam: Implications for the early Paleozoic assembly of the Indochina Block. Gondwana Research, 2019, 70, 151-170.	6.0	49
29	Intensified continental chemical weathering and carbon-cycle perturbations linked to volcanism during the Triassic–Jurassic transition. Nature Communications, 2022, 13, 299.	12.8	49
30	Increased productivity as a primary driver of marine anoxia in the Lower Cambrian. Palaeogeography, Palaeoclimatology, Palaeoecology, 2018, 491, 1-9.	2.3	48
31	The spatial (nearshore–offshore) distribution of latest Permian phytoplankton from the Yangtze Block, South China. Palaeogeography, Palaeoclimatology, Palaeoecology, 2012, 363-364, 151-162.	2.3	42
32	Neoarchean and Paleoproterozoic K-rich granites in the Phan Si Pan Complex, north Vietnam: Constraints on the early crustal evolution of the Yangtze Block. Precambrian Research, 2019, 332, 105395.	2.7	42
33	Zircon U-Pb geochronological evidence for the evolution of the Nan-Uttaradit suture in northern Thailand. Journal of Earth Science (Wuhan, China), 2016, 27, 378-390.	3.2	41
34	Late Triassic post-collisional granites related to Paleotethyan evolution in SE Thailand: Geochronological and geochemical constraints. Lithos, 2017, 286-287, 440-453.	1.4	41
35	Origin of Permian OIB-like basalts in NW Thailand and implication on the Paleotethyan Ocean. Lithos, 2017, 274-275, 93-105.	1.4	40
36	Clay mineralogical characteristics at the Permian–Triassic Shangsi section and their paleoenvironmental and/or paleoclimatic significance. Palaeogeography, Palaeoclimatology, Palaeoecology, 2017, 474, 152-163.	2.3	37

#	Article	IF	CITATIONS
37	Discovery of a Late Devonian magmatic arc in the southern Lancangjiang zone, western Yunnan: Geochemical and zircon U–Pb geochronological constraints on the evolution of Tethyan ocean basins in SW China. Journal of Asian Earth Sciences, 2016, 118, 32-50.	2.3	36
38	CHANGXINGIAN (UPPER PERMIAN) RADIOLARIAN FAUNA FROM MEISHAN D SECTION, CHANGXING, ZHEJIANG, CHINA, AND ITS POSSIBLE PALEOECOLOGICAL SIGNIFICANCE. Journal of Paleontology, 2005, 79, 209-218.	0.8	35
39	An eukaryote-bearing microbiota from the early mesoproterozoic Gaoyuzhuang Formation, Tianjin, China and its significance. Precambrian Research, 2017, 303, 709-726.	2.7	35
40	TAXONOMY OF ORDER LATENTIFISTULARIA (RADIOLARIA) FROM THE LATEST PERMIAN IN SOUTHERN GUANGXI, CHINA. Journal of Paleontology, 2006, 80, 826-848.	0.8	34
41	Early Paleoproterozoic magmatism in the Yangtze Block: Evidence from zircon U-Pb ages, Sr-Nd-Hf isotopes and geochemistry of ca. 2.3†Ga and 2.1†Ga granitic rocks in the Phan Si Pan Complex, north Vietnam. Precambrian Research, 2019, 324, 253-268.	2.7	34
42	Petrogenesis of Archean TTGs and potassic granites in the southern Yangtze Block: Constraints on the early formation of the Yangtze Block. Precambrian Research, 2020, 347, 105848.	2.7	34
43	A LATE PERMIAN TO EARLY TRIASSIC BIVALVE FAUNA FROM THE DONGPAN SECTION, SOUTHERN GUANGXI, SOUTH CHINA. Journal of Paleontology, 2007, 81, 1009-1019.	0.8	33
44	UPPERMOST CHANGXINGIAN (PERMIAN) RADIOLARIAN FAUNA FROM SOUTHERN GUIZHOU, SOUTHWESTERN CHINA. Journal of Paleontology, 2002, 76, 797.	0.8	32
45	Tracing the provenance of volcanic ash in Permian–Triassic boundary strata, South China: Constraints from inherited and syn-depositional magmatic zircons. Palaeogeography, Palaeoclimatology, Palaeoecology, 2019, 516, 190-202.	2.3	31
46	Volcanically induced environmental change at the Permian–Triassic boundary (Xiakou, Hubei) Tj ETQq0 0 0 rgB Sciences, 2013, 75, 95-109.	T /Overloc 2.3	2k 10 Tf 50 3 30
47	Phylogenetic model of <i>Follicucullus</i> lineages (Albaillellaria,) Tj ETQq1 1 0.78 South China. Journal of Micropalaeontology, 2014, 33, 179-192.	4314 rgBT 3.6	7 /Overlock 30
48	Petrogenesis and tectonic implication of the Late Triassic post-collisional volcanic rocks in Chiang Khong, NW Thailand. Lithos, 2016, 248-251, 418-431.	1.4	30
49	The Ediacaran-Cambrian rise of siliceous sponges and development of modern oceanic ecosystems. Precambrian Research, 2019, 333, 105438.	2.7	30
50	Long-lived Paleotethyan pelagic remnant inside Shan-Thai Block: Evidence from radiolarian biostratigraphy. Science in China Series D: Earth Sciences, 2004, 47, 1113-1119.	0.9	29
51	Paleoproductivity and paleoredox condition of the Huai Hin Lat Formation in northeastern Thailand. Journal of Earth Science (Wuhan, China), 2016, 27, 350-364.	3.2	28
52	Geochronological and geochemical constraints on the intermediate-acid volcanic rocks along the Chiang Khong–Lampang–Tak igneous zone in NW Thailand and their tectonic implications. Gondwana Research, 2017, 45, 87-99.	6.0	28
53	The Permian seamount stratigraphic sequence in Chiang Mai, North Thailand and its tectogeographic significance. Science in China Series D: Earth Sciences, 2008, 51, 1768-1775.	0.9	27
54	Geochemistry of Triassic siliceous rocks of the Muyinhe Formation in the Changning-Menglian belt of Southwest China. Journal of Earth Science (Wuhan, China), 2016, 27, 403-411.	3.2	27

#	Article	IF	CITATIONS
55	A late Changhsingian (latest Permian) radiolarian fauna from Chaohu, Anhui and a comparison with its contemporary faunas of South China. Alcheringa, 2008, 32, 199-222.	1.2	26
56	High-resolution clay mineral and major elemental characterization of a Permian-Triassic terrestrial succession in southwestern China: Diagenetic and paleoclimatic/paleoenvironmental significance. Palaeogeography, Palaeoclimatology, Palaeoecology, 2017, 481, 77-93.	2.3	26
57	Uppermost Changxingian (Permian) radiolarian fauna from southern Guizhou, southwestern China. Journal of Paleontology, 2002, 76, 797-809.	0.8	25
58	Petrochemistry and tectonic setting of the Middle Triassic arc-like volcanic rocks in the Sayabouli area, NW Laos. Journal of Earth Science (Wuhan, China), 2016, 27, 365-377.	3.2	24
59	Geochemical and geochronological constrains on the Chiang Khong volcanic rocks (northwestern) Tj ETQq1 1	0.784314 r 2.1	gBT_/Overlock
60	Palaeoenvironmental implications of geochemistry and radiolarians from Upper Devonian chert/shale sequences of the Truong Son fold belt, Laos. Geological Journal, 2017, 52, 154-173.	1.3	22
61	The link between metazoan diversity and paleo-oxygenation in the early Cambrian: An integrated palaeontological and geochemical record from the eastern Three Gorges Region of South China. Palaeogeography, Palaeoclimatology, Palaeoecology, 2018, 495, 24-41.	2.3	22
62	New probable cnidarian fossils from the lower Cambrian of the Three Gorges area, South China, and their ecological implications. Palaeogeography, Palaeoclimatology, Palaeoecology, 2018, 505, 150-166.	2.3	22
63	ALBAILLELLIDAE (RADIOLARIA) FROM THE LATEST PERMIAN IN SOUTHERN GUANGXI, CHINA. Journal of Paleontology, 2007, 81, 9-18.	0.8	21
64	The diversity of the Permian phytoplankton. Review of Palaeobotany and Palynology, 2013, 198, 145-161.	1.5	21
65	Proto-Tethys ophiolitic mélange in SW Yunnan: Constraints from zircon U-Pb geochronology and geochemistry. Geoscience Frontiers, 2021, 12, 101200.	8.4	21
66	Permian andÂTriassic Radiolaria from Northwest Thailand: paleogeographical implications. Revue De Micropaleontologie, 2005, 48, 237-255.	0.4	20
67	The prelude of the end-Permian mass extinction predates a postulated bolide impact. International Journal of Earth Sciences, 2007, 96, 903-909.	1.8	20
68	Geochronological and Geochemical Constraints on the Petrogenesis of Early Paleoproterozoic (2.40-2.32 Ga) Nb-Enriched Mafic Rocks in Southwestern Yangtze Block and Its Tectonic Implications. Journal of Earth Science (Wuhan, China), 2020, 31, 35-52.	3.2	20
69	End-Permian conodont fauna from Dongpan section: Correlation between the deep-and shallow-water facies. Science in China Series D: Earth Sciences, 2008, 51, 1611-1622.	0.9	19
70	Geochemical constraints on the depositional environment of Upper Devonian radiolarian cherts from Loei, north-eastern Thailand. Frontiers of Earth Science, 2011, 5, 178-190.	2.1	19
71	A latest Permian radiolarian fauna from Hushan, South China, and its geological implications. Alcheringa, 2011, 35, 471-496.	1.2	19
72	Changhsingian radiolarian fauna from Anshun of Guizhou, and its relationship to TOC and paleo-productivity. Science China Earth Sciences, 2013, 56, 1334-1342.	5.2	19

#	Article	IF	CITATIONS
73	Latest Permian acritarchs from South China and theMicrhystridium/Veryhachiumcomplex revisited. Palynology, 2013, 37, 325-344.	1.5	19

- Geochemistry, zircon U-Pb age and Hf isotopic constraints on the petrogenesis of the Silurian rhyolites in the Loei fold belt and their tectonic implications. Journal of Earth Science (Wuhan,) Tj ETQq0 0 0 rgBT / @ relock 100 Tf 50 69 74

75	Zircon U–Pb geochronology, and elemental and Sr–Nd–Hf–O isotopic geochemistry of post-collisional rhyolite in the Chiang Khong area, NW Thailand and implications for the melting of juvenile crust. International Journal of Earth Sciences, 2017, 106, 1375-1389.	1.8	19
76	An illustrated catalogue and revised classification of paleozoic radiolarian genera. Geodiversitas, 2017, 39, 363-417.	0.8	18
77	New Siliceous Microfossils from the Terreneuvian Yanjiahe Formation, South China: The Possible Earliest Radiolarian Fossil Record. Journal of Earth Science (Wuhan, China), 2018, 29, 912-919.	3.2	18
78	Carbonate carbon isotope chemostratigraphy and U-Pb zircon geochronology of the Liuchapo Formation in South China: Constraints on the Ediacaran-Cambrian boundary in deep-water sequences. Palaeogeography, Palaeoclimatology, Palaeoecology, 2019, 535, 109361.	2.3	18
79	Timing of the terrestrial Permian-Triassic boundary biotic crisis: Implications from U-Pb dating of authigenic zircons. Science in China Series D: Earth Sciences, 2008, 51, 1633-1645.	0.9	16
80	Radiolarian Kalimnasphaera from the Cambrian Shuijingtuo Formation in South China. Marine Micropaleontology, 2014, 110, 3-7.	1.2	16
81	Biotic evolution and its relation with geological events in the Proterozoic Yanshan Basin, North China. Science China Earth Sciences, 2014, 57, 903-918.	5.2	16
82	Radiolarian fauna from the Chiungchussuan Shuijingtuo Formation (Cambrian Series 2) in Western Hubei Province, South China. Science China Earth Sciences, 2019, 62, 1645-1658.	5.2	16
83	Some New Radiolarian Species and Genus from Upper Permian in Guangxi Province, South China. Journal of Paleontology, 2010, 84, 879-894.	0.8	15
84	On the Lower Cambrian biotic and geochemical record of the Hetang Formation (Yangtze Platform,) Tj ETQq0 0 Micropalaeontology, 2013, 32, 207-217.	0 rgBT /O [.] 3.6	verlock 10 ⁻ 15
85	Chert-hosted small shelly fossils: expanded tool of biostratigraphy in the Early Cambrian. Gff, 2014, 136, 303-308.	1.2	15
86	Source of silica and silicification of the lowermost Cambrian Yanjiahe Formation in the Three Gorges area, South China. Palaeogeography, Palaeoclimatology, Palaeoecology, 2020, 548, 109697.	2.3	15
87	Tracking Prototethyan assembly felsic magmatic suites in southern Yunnan (SW China): evidence for an Early Ordovician–Early Silurian arc–back-arc system. Journal of the Geological Society, 2021, 178, .	2.1	14
88	Early Carboniferous radiolarians from north-west Thailand: palaeogeographical implications. Palaeontology, 2004, 47, 377-393.	2.2	13
89	Late Changhsingian radiolarian biostratigraphy from Guangxi, South China and its correlation to conodonts. Science in China Series D: Earth Sciences, 2008, 51, 1601-1610.	0.9	13
90	Silicon isotopes reveal a decline in oceanic dissolved silicon driven by biosilicification: A prerequisite for the Cambrian Explosion?. Earth and Planetary Science Letters, 2021, 566, 116959.	4.4	13

#	Article	IF	CITATIONS
91	Geochemistry of Middle Triassic radiolarian cherts from northern Thailand: Implication for depositional environment. Journal of Earth Science (Wuhan, China), 2011, 22, 688-703.	3.2	12
92	Petrography, geochemistry and U-Pb detrital zircon dating of the clastic Phu Khat Formation in the Nakhon Thai region, Thailand: Implications for provenance and geotectonic setting. Journal of Earth Science (Wuhan, China), 2016, 27, 329-349.	3.2	12
93	Permian radiolarian biostratigraphy. Geological Society Special Publication, 2018, 450, 143-163.	1.3	12
94	Geochronological and geochemical constraints on the petrogenesis of late Mesoproterozoic mafic and granitic rocks in the southwestern Yangtze Block. Geoscience Frontiers, 2021, 12, 39-52.	8.4	12
95	Extinction pattern and process of siliceous sponge spicules in deep-water during the latest Permian in South China. Science in China Series D: Earth Sciences, 2008, 51, 1623-1632.	0.9	11
96	Integrated radiolarian and conodont biostratigraphy of the Middle Permian Gufeng Formation (South) Tj ETQq0 (0 0 rgBT /0	Overlock 10
97	New Insight into Factors Controlling Organic Matter Distribution in Lower Cambrian Source Rocks: A Study from the Qiongzhusi Formation in South China. Journal of Earth Science (Wuhan, China), 2020, 31. 181-194.	3.2	11

98	Phytoplankton (acritarch) community changes during the Permian-Triassic transition in South China. Palaeogeography, Palaeoclimatology, Palaeoecology, 2019, 519, 84-94.	2.3	10
99	Permian radiolarians, chert and basalt from the Daxinshan Formation in Lancangjiang belt of southwestern Yunnan, China. Science in China Series D: Earth Sciences, 2002, 45, 63-71.	0.9	9
100	Late Changhsingian (Latest Permian) radiolarians from Chaohu, Anhui. Journal of Earth Science (Wuhan, China), 2009, 20, 797-810.	3.2	9
101	Geochemistry of radiolarian cherts from a Late Devonian continental margin basin, Loei fold belt, Indo-China terrane. Journal of Earth Science (Wuhan, China), 2017, 28, 29-50.	3.2	9
102	Microbial and animal evolution in relation to redox fluctuations in a deep-water setting of South China during the Ediacaran-Cambrian transition (ca. 551–523ÂMa). Palaeogeography, Palaeoclimatology, Palaeoecology, 2020, 546, 109672.	2.3	9
103	Study on the geochemical characteristics of ocean-ridge and oceanic-island volcanic rocks in the Nan-Uttaradit zone, northern Thailand. Diqiu Huaxue, 2010, 29, 175-181.	0.5	8
104	Uneven Distribution of <i>Pseudotormentus</i> De Wever et Caridroit (Radiolaria, Protozoa): Provincialism of a Permian Planktonic Microorganism. Acta Geologica Sinica, 2016, 90, 1598-1610.	1.4	7
105	Middle Triassic radiolarians from cherts/siliceous shales in an extensional basin in the Sukhothai fold belt, Northern Thailand. Journal of Earth Science (Wuhan, China), 2017, 28, 9-28.	3.2	6
106	Recent achievements on the research of the Paleozoic-Mesozoic transitional period in South China. Frontiers of Earth Science, 2007, 1, 129-141.	0.5	5
107	High-resolution cyclostratigraphy of geochemical records from Permo-Triassic boundary section of Dongpan, southwestern Guangxi, South China. Science in China Series D: Earth Sciences, 2008, 51, 187-193.	0.9	5
108	Influence of palaeo-redox and diagenetic conditions on the spatial distribution of Cambrian biotas: A case study from the upper Shuijingtuo Formation (Cambrian Series 2, Stage 3), Three Gorges area of South China. Palaeogeography, Palaeoclimatology, Palaeoecology, 2020, 548, 109696.	2.3	5

#	Article	IF	CITATIONS
109	Microfossil Assemblages and Indication of the Source and Preservation Pattern of Organic Matter from the Early Cambrian in South China. Journal of Earth Science (Wuhan, China), 2022, 33, 802-819.	3.2	5
110	Geochemical characteristics of island-arc volcanic rocks in the Nan-Nam Pat-Phetchabun zone, northern Thailand. Diqiu Huaxue, 2010, 29, 337-342.	0.5	4
111	Palaeoecological assemblages of the lower Cambrian Shuijingtuo Biota from the three Gorges area and implications for co-evolution of environments and life. Palaeogeography, Palaeoclimatology, Palaeoecology, 2021, 566, 110193.	2.3	4
112	Microfossils from the Liuchapo Formation: Possible oldest radiolarians from deep-water chert and phylogenetic analysis. Precambrian Research, 2021, 362, 106312.	2.7	4
113	Cloudina aggregates from the uppermost Dengying Formation, Three Gorges area, South China, and stratigraphical implications. Precambrian Research, 2022, 370, 106552.	2.7	4
114	Deep-water fossil assemblages from the Ediacaran-Cambrian transition of western Hunan, South China and their biostratigraphic and evolutionary implications. Palaeogeography, Palaeoclimatology, Palaeoecology, 2022, 591, 110878.	2.3	4
115	Depositional characteristics of Dalong Formation and its potential as hydrocarbon source rocks in Hubei, Hunan, Guizhou and Guangxi. Frontiers of Earth Science, 2007, 1, 452-457.	0.5	3
116	Tracing escaping structure in the Northern Indo-China Peninsula by Openness and remote sensing. Journal of Earth Science (Wuhan, China), 2017, 28, 147-160.	3.2	3
117	Editorial: The co-evolution of life and environments in South China from Snowball Earth to Cambrian Explosion. Palaeogeography, Palaeoclimatology, Palaeoecology, 2021, 563, 110181.	2.3	3
118	Morphological characteristics of a dimorphic pair of <i>Albaillella sinuata</i> Ishiga and Watase: Dimorphism in the lineage of the Permian Albaillellaria (Radiolaria). Island Arc, 2018, 27, e12271.	1.1	2
119	Diverse cuticular remains in Cambrian (Series 2) SSF assemblages from China and the pioneer metazoan colonization of offshore environments. Palaeogeography, Palaeoclimatology, Palaeoecology, 2021, 567, 110192.	2.3	2
120	Integrated Radiolarian and Conodont Biostratigraphy of the Middle to Late Permian Linghao Formation in Northwestern Guangxi, South China. Acta Geologica Sinica, 0, , .	1.4	2
121	The Guadalupian (Permian) Gufeng Formation on the North Margin of the South China Block: A Review of the Lithostratigraphy, Radiolarian Biostratigraphy, and Geochemical Characteristics. Paleontological Research, 2019, 23, 261.	1.0	2
122	Geochemical characteristics of the oceanic island-type volcanic rocks in the Chiang Mai zone, northern Thailand. Diqiu Huaxue, 2009, 28, 258-263.	0.5	1
123	The boundary between the Inthanon Zone (Palaeotropics) and the Gondwana-derived Sibumasu Terrane, northwest Thailand—evidence from Permo-Triassic limestones and cherts. Palaeobiodiversity and Palaeoenvironments, 2022, 102, 383-418.	1.5	1
124	Fossil evidence provides new insights into the origin of the Mesoproterozoic ministromatolites. Precambrian Research, 2021, 366, 106426.	2.7	0
125	New Radiolarian Genus Ganjiangmoyea gen. nov. from the Lopingian (Upper Permian) in Guangxi, South China. Paleontological Research, 2019, 23, 281.	1.0	0